

# Low mass variable stars in the globular cluster NGC 6397

E. Martinazzi<sup>1,2\*</sup>, S. O. Kepler<sup>1</sup>, J. E. S. Costa<sup>1</sup>

<sup>1</sup>*Instituto de Física, Universidade Federal do Rio Grande do Sul, 91501-900 Porto Alegre, RS, Brazil*

<sup>2</sup>*Instituto Federal do Rio Grande do Sul, 95700-000, Bento Gonçalves, RS, Brazil*

Accepted Received XXX XXX XXX

## ABSTRACT

We have conducted a photometric survey of the globular cluster NGC 6397 in a search for variable stars. We obtained  $\sim 11$  h of time-resolved photometric images with one new European Southern Observatory-Very Large Telescope using the FOcal Reducer and low dispersion Spectrograph imager distributed over two consecutive nights. We analyzed 8 391 light curves of stars brighter than magnitude 23 with the 465 nm-filter, and we identified 412 variable stars, reaching  $\sim 4.8 \pm 0.2$  per cent of variability with timescales between 0.004 and 2 d, with amplitudes variation greater than  $\pm 0.2$  mag.

**Key words:** convection methods: data analysis techniques: photometric stars: chromo-spheres stars: low-mass stars: variables: general.

## 1 INTRODUCTION

Stellar variability depends on effective temperature, magnetic field and also on the opacity, which is metallicity dependent. Globular clusters offers a way to study this dependence. As globular cluster are some of the oldest objects in the Universe, they are laboratories for the study of the early stages of Galaxy formation (e.g. Binney & Merrifield 1998; Freeman & Bland-Hawthorn 2002). Each cluster is made up by a essentially simple population of stars, i.e. practically all stars were born from the same molecular cloud (e.g. Rosenberg et al. 2000) even though there is evidence for multiple populations in a few clusters. The comparison between the ratio of variable M stars in function of their masses for globular clusters with different metallicities and the ratio for the galactic disk can tell us whether metallicity plays an important role at low temperatures.

The globular cluster NGC 6397 is particularly interesting in this context. NGC 6397 is a globular relatively easy to study due to its proximity. It is considered, together with NGC 6101 (M4), one of the two nearest clusters from the Sun, located at a distance  $R_{SS} = 2.2^{+0.5}_{-0.7}$  kpc (Heyl 2012) at  $\alpha = 17^{\text{h}} 40^{\text{m}} 42.09^{\text{s}}$  and  $\delta = -53^{\circ} 40' 27.6''$  (J2000), with galactocentric coordinates  $\ell = 338.17^{\circ}$  and  $b = -11.96^{\circ}$ . NGC 6397 is classified as a core-collapsed cluster, predicted by theory decades ago and confirmed by observations (Trager et al. 1995; Martinazzi et al. 2014). The distance moduli for NGC 6397 is  $12.02 \pm 0.06$  (Hansen et al. 2007) with reddening  $E(B-V) = 0.18 \pm 0.02$  [Harris (1996) 2010 edition]. Another remarkable feature of NGC 6397 is

its low metallicity. In fact, it is one of the lowest metallicity globular clusters known, with  $[Fe/H] = -1.99 \pm 0.02$  (Carretta et al. 2009).

Kaluzny (1996) reported five new variable stars, including SX Phe stars and RR Lyrae variables. Kaluzny (1997) reported that few variable stars are known in the globular cluster NGC 6397. They obtained light curves for seven additional discoveries, identified as close binaries, SX Phe stars and RR Lyrae variable. Kaluzny & Thompson (2003), studied the central region of NGC 6397 and detected nine new variables stars, including one eclipsing binary, new SX Phe stars and low amplitude variables. Kaluzny et al. (2006) presented 12 new objects, of which six are periodic light curves and eclipsing binaries of unknown period again in the central region of the cluster.

Cohn et al. (2010) studied X-ray sources identified by the Chandra telescope near the center of the cluster. In addition to studying nine cataclysmic variables (CVs) previously detected, they identified six new weak candidates for CV. Nascimbeni et al. (2012) conducted a search for variables and planetary transits in NGC 6397, exploring the images of the HST (Hubble Space Telescope). They analyzed 5 078 light curves, including a selection of 2 215 cluster-member M dwarfs selected on the proper motions and reported 12 new variable stars. The great majority of the variables previously known are in the central region of the cluster.

The main objective of this work is to determine the variable star ratio as a function of mass for NGC 6397, studying if the variability is related to the metallicity.

\* E-mail: elizandra.martinazzi@ufrgs.br

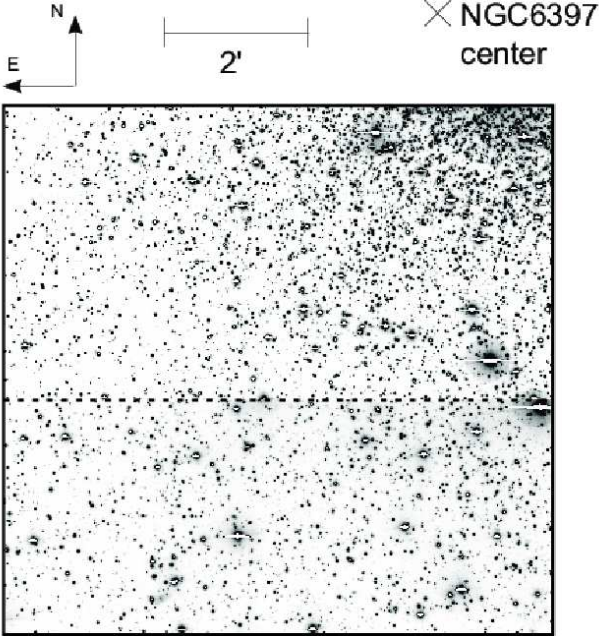


**Figure 1.** CCDs images of the NGC 6397, CCD1 in the top and CCD2 in the bottom. The dotted line indicates the border between both CCDs. The top edge of the right CCD1 is distant  $\sim 1'$  from the cluster center ( $0, 72\text{ pc}$ ).

## 2 OBSERVATIONAL DATA AND DATA REDUCTION

The images used in this work were obtained from the ESO program ID 083.D-0653(A) P.I. Barbara Castanheira. They were taken in 2009 July 27-28, with 8.4-m ESO-VLT-UT1 telescope (*Very Large Telescope*), using the FORS2 (*Focal Reducer and low dispersion Spectrograph*) imager composed by two CCDs with a total of  $2048 \times 2068$  pixels and  $0.25''/\text{pixel}$  scale, with an usable portion total of  $1670 \times 1677$  pixels.

The images are taken with the filter FILT\_465\_250 (central wavelength  $\lambda=4650\text{ \AA}$  and  $\Delta\lambda=250\text{ \AA}$ ). A total of 305 images were obtained: 205 of 60 s on the first night, 28 of 80 s on the first part of the second night and 72 images of 170 s on the second part of the last night, starting at Julian date JD = 2 455 038.507350.

We obtained 5.1 h of photometry on the first night and 4.8 h on the second night, with a separation of 19.95 h. The CCD reading time was of the order of 30 s. CCD1 covers a  $6, 8' \times 3, 9'$  field and CCD2  $6, 8' \times 2, 9'$  field, amounting to  $6, 8' \times 6, 8'$  the whole field, without any gap between the CCDs. The images were centred at  $\alpha = 17h\,41m\,01.78s$  and  $\delta = -53^\circ 44' 47.2''$  (J2000). The cluster centre, excluded from the images, is around 1.1 arcmin to the upper right corner of the CCD1 (Fig. 1).

Image data reduction were carried out with standard IRAF routines, with tasks *daofind*, *phot* and *allstar*, applying Point Spread Function (PSF) photometric procedures. The astrometric calibration was done using the coordinates of the white dwarfs studied by Moehler et al. (2000). The images were centered on R.A. =  $17h\,41min\,01,65\text{ s}$  e DEC. =  $-53^\circ 44' 46,05''$  (J2000) to cover the region where the white

dwarf candidates for DAVs. The correction for atmospheric extinction for a given filter was applied from the equation  $m_0 = ZP + m - KX$ , where  $m_0$  is the corrected apparent magnitude,  $m$  is the apparent instrumental magnitude,  $ZP$  is the zero point,  $X \simeq \sec(z)$ , the air mass, which varies throughout the night, depending on the zenithal distance  $z$  of the object.

To create a reference magnitude data and subtract from the measured magnitudes for a given image, we compared the instrumental magnitude with the apparent magnitude of twenty standard cluster stars and determine a  $ZP$  for each image. This procedure is equivalent to assuming that  $ZP$  is constant and  $K$  undergoes fluctuations over time. For the photometric calibration, we use the standard stars in the same field, measured by Stetson (2000) and Stetson et al. (2005). After we applied the photometric corrections we obtained the light curves of each star, where each point of the light curve is the apparent magnitude calculated photometrically by PSF fitting. The extinction coefficient for the filter FILT\_465\_250 was calculated from an interpolation of tabulated values. The mean value assumed for this filter was  $K = 0.189$ . The average seeing was  $1.18''$  for the first night and  $0.69''$  for the second night. We included, in the calculations, the effect of the uncertainties in the instrumental magnitude, the zero point and the air mass.

We built the color-magnitude diagram (CMD) shown in Fig. 2 from images obtained with B\_HIGH and V\_HIGH filters, with exposure times of 1, 10, 120, 300 s each, and 1, 300 or 600 s with U\_HIGH filter. The data reduction were performed using IRAF routines, with the tasks *daofind*, *phot* and *allstar*, applying standard point spread function photometric procedures. The best-fitting PSF function among those available was the elliptical Moffat with coefficient  $\beta = 2.5$ . Objects brighter than V\_HIGH filter  $\simeq 19$  were saturated in the 300 s images. Two lists of positions were created for each CCD using the images of 1 s (V\_HIGH filter) for the brightest stars and 300 s (V\_HIGH filter) for the faint stars and both data sets were combined to avoid superposition.

In order to exclude probable non-member objects as the field stars, we use a colour-magnitude filter applied to the CMD built with the ESO-VLT data. This procedure eliminated  $\sim 25$  per cent of the stars originally present in the CMD of NGC 6397. In Martinazzi et al. (2014) the luminosity and density of Milky Way field stars in the direction of NGC 6397 were estimated, obtaining a contamination by Galactic stars of  $0.04\text{ stars/arcsec}^2$ . The cut is shown in Fig. 2 at the right side CMD.

We found 7617 objects in CCD1 and 3739 in CCD2, totalling 11 356 objects in the whole field with magnitudes between 15 and 25. However, for stars brighter than magnitude 23 in the 465nm-filter, we find a total 8 391 stars. This range of magnitude was selected because fainter stars than magnitude 23 were contaminated by the large brightness variation of the sky (zodiacal light, even without moon) as shown in Fig. 3. We only used light curves for stars detected in more than 100 images. We also eliminate the stars near the edge of images, over a distance of 15 pixels from the edges.

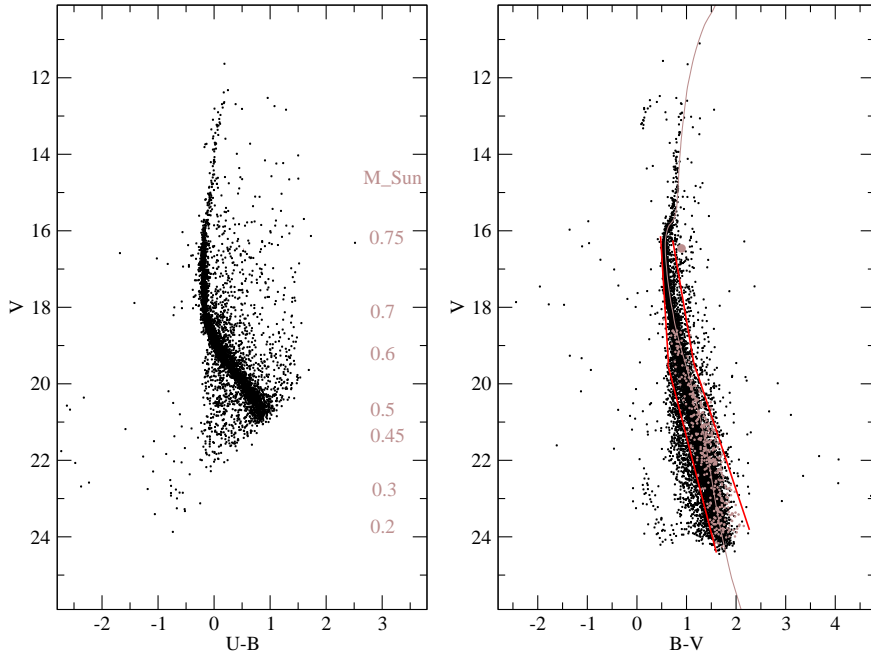


**Figure 2.** NGC 6397 color-magnitude diagram for the data of this work. The values shown in the left panel represent the approximate position of the masses obtained by isochrones, line in the right panel, calculated by A. Dotter (2008) to the lower limit of the burning of H. The lines at the right side CMD shown the colour-magnitude filter applied in order to exclude probable non-member objects as the field stars.

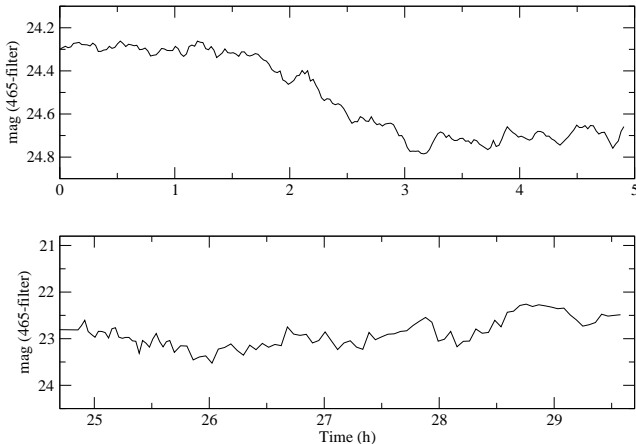


**Figure 3.** Brightness variation of the sky during both observation evenings in the 465nm-filter. In the first night (top) we used exposure time of 60 s. In the second night (bottom), we used 80 s in the first part and 170 s in second part of the observations.

### 3 LOW MASS VARIABLE STARS

The M dwarfs are the most numerous stars in the Galaxy (e.g. Rojas-Ayala et al. 2014). The understanding of the inner structure of the largest population of stars in our Galaxy could occur through observations of pulsating M dwarfs. Rodríguez-López et al. (2014) presented a theoretical study of the instability strip of M dwarf stars for models in the range  $0.10 - 0.60 M_{\odot}$ , with model for different metallicity in the range  $-1.0 < [Fe/H] < 0.0$ , showing theoretical evidence that solar-like oscillations can be excited in these stars. They found that the M dwarfs unstable modes have periods rang-

ing from 0.014 - 0.46 d depending on the mass and evolutionary stage.

Solar-like oscillations have small amplitudes, but variations were observed to be stronger than predicted in the planning by the Kepler satellite (Gershberg 2005). Manifestations of the activity of lower main-sequence stars are numerous and diverse. Sporadic flares are observed in all layers of the stellar atmosphere, as well as cool spots involving the stellar surface and manifesting variability of large-scale structures in stellar atmospheres, chromospheres and coronae (Gershberg 2005). All these effects could have longer timescale than we studied.

Hartman et al. (2011) investigated the optical broadband photometric variability of a sample of 27 560 field K and M dwarfs selected by color and proper motion using light curves from the HATNet survey for transiting extrasolar planets. They searched the light curves for periodic variations and for large-amplitude, long-duration flare events totalling 2 120 stars with potential variability using time-bases between 45 days and 2.5 years. They also found that the rotation periods and amplitudes of K and early-to mid-M dwarfs are uncorrelated for periods less than 30 days, and that amplitude decreases with increasing rotation period greater than 30 days. The majority of the variables are BY Dra type main-sequence stars, usually K or M, exhibiting variations due to rotation coupled with star spots and other chromospheric activity. They investigate the relations between period, color, age, and activity measures, including optical flaring, for K and M dwarfs and determined that the fraction of stars that is variable with amplitudes greater than 0.01 mag and periods between 0.1 and 100 days, increases exponentially such that  $\sim 50$  per cent of field dwarf

stars in the solar neighbourhood are variable at this level and at these timescales.

Schmidt et al. (2014) presented the colours and activity of ultra-cool dwarfs from the Tenth Data Release of the Sloan Digital Sky Survey (SDSS) combining the previous samples of SDSS M and L dwarfs with new data obtained from the Baryon Oscillation Sky Survey (BOSS) to produce the BOSS Ultra-cool Dwarf (BUD) sample of 11 820 dwarfs. They obtained the fraction of active dwarfs rises through the M spectral sequence until it reaches  $\sim 90$  per cent at spectral type L0, through the presence of H $\alpha$  emission. The fraction of active dwarfs then declines to 40 per cent at spectral type M5 (mass  $\sim 0.21 M_{\odot}$ , by the Drilling & Landolt (2000) classification). Considering M dwarfs only within 100 pc from the Galactic plane, the activity fraction increases to 10 per cent at type M0 (mass  $\sim 0.51 M_{\odot}$ ) and 50 per cent at type M4.

On the other hand, several studies of the low mass stars have been performed by the *Kepler* mission - a space telescope whose principal purpose was to detect transits and to discover exoplanets, that provides an great opportunity to study the light-curves of stars with never before studied precision and coverage. In the first look at a large sample of stars with photometric data of a quality that has heretofore been only available for our Sun, Basri et al. (2010) found that nearly half of their sample was more active than the active Sun.

Newton et al. (2015) using photometry from the MEarth transit survey detected rotation periods between 0.1 and 150 days for 391 nearby mid-to-late M dwarfs in the Northern hemisphere. For fully-convective stars with detected rotation periods, they found no correlation between metallicity and rotation period or amplitude.

Estimating M dwarf rotation periods, West et al. (2015) used photometric observations from the Earth survey for transiting exoplanets. Using spectroscopic observations and photometric light curves of 238 nearby M dwarfs, they examined the relationships between magnetic activity by H $\alpha$  emission, rotation period, and stellar age. The amplitude of the photometric modulations detected were typically 0.5 to 2% peak-to-peak. For all M spectral types, they found that the presence of magnetic activity is tied to rotation, including for late-type, fully convective M dwarfs.

## 4 VARIABLE STARS

For each light curve calculate the *chi-square*,

$$\chi^2 = \sum_{i=1}^N \left( \frac{m_i - \bar{m}}{\sigma_i} \right)^2 , \quad (1)$$

where,  $m_i$  and  $\sigma_i$  are the  $i^{th}$  magnitude measure and its uncertainty and  $\bar{m}$  the average magnitude. Both stellar variability and underestimated uncertainties can lead to high values of  $\chi^2$ . On other hand, overestimated uncertainties can lead to low values for  $\chi^2$ . The probability of a *chi-square* distribution with  $(N - 1)$  degrees of freedom have a value less than  $\chi^2$  by chance can be calculated directly from the *chi-square* cumulative distribution function. Figure 5 shows the calculated probabilities in function of the magnitude for the 9 868 stars found in our NGC 6397 images. The Fig. 4

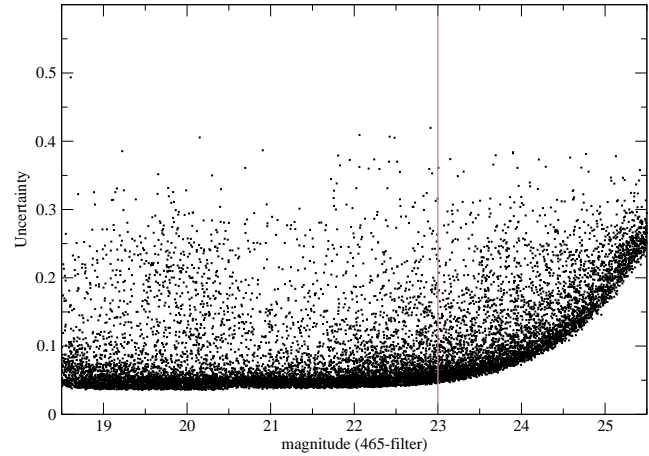


**Figure 4.** Uncertainty as the function of the magnitude in the 465-filter. The vertical line shows the magnitude limit used in this work.

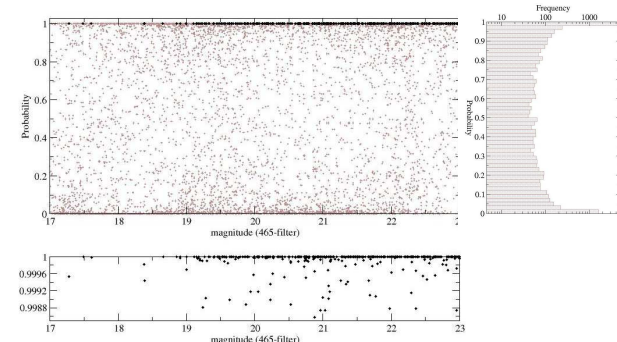


**Figure 5.** Distribution of probability of variability in the 465nm-filter of NGC 6397 stars. The stars selected as candidates for variables have confidence level of 99.9%, with amplitudes variation greater than  $\pm 0.2$  magnitude. The top shows all the 9 868 stars studied. Bottom panel shows a zoom of the region with probability above 99.9%, containing 412 variable stars. The right panel shows frequency of the probability distribution function of the number of stars.

shows the uncertainty as function of the magnitude in the 465-filter, which was used in Equation 1.

After sorting by the probability and  $\chi^2$  variability method, those that showed variability in one or both the nights with amplitude variation greater than 0.2 mag were selected. However, it was necessary to make a visual inspection of the light curve to remove false alarms, discarding more than half of the candidates. Examples of candidate variables are selected stars shown in Fig. 6 (a), (b) and (c). A light curve of a star considered normal or not variable, is shown in (d) Fig. 6. More than half of the stars selected as candidates for variables were false alarms due to contamination of diffraction rays of bright stars, as the example shown in (e) Fig. 6, or large brightness variation of the estimated background.

We found a total of 412 variables stars with 99.9% confidence level, corresponding to  $4.8 \pm 0.2$  per cent of the observed stars between between magnitude 17 and 23 in the 465nm-filter. The objects brighter than  $V \simeq 17$  were satu-

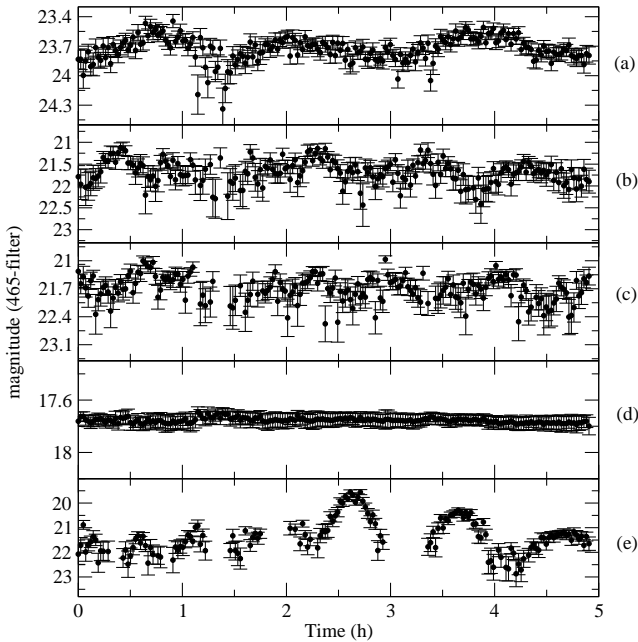


**Figure 6.** Panels (a), (b) and (c) are examples of light curve selected as variable stars; (d) is a typical light curve of a normal star, while (e) is an example of light curve with contamination by diffraction rays of a neighbour star brightness, eliminated by visual inspection.

rated, so it was not possible in this study, to search for some rapidly rotating stars, contact binaries, RR Lyrae, or SX Phe stars. Fig. 7 shows the positions of variables (circles) in images obtained with the ESO-VLT.

Figure 8 shows the histogram of not variable stars and the magnitude compared with the number of variables stars candidate and Figure 9 shows the fraction of variables as a function of the stellar mass for NGC 6397 with magnitude between 17 and 23 (465nm-filter).

The cold stars located in the lower main sequence commonly present high chromospheric activity and will have spots on their surfaces (e.g. Valio 2012). Convection is an important form of the transport of energy and momentum in stellar interiors. For low-temperature stars with extended convective envelope, convection exceed radiation and becomes the major form of energy transportation (e.g. Xiong et al. 2016). The active fraction peaks at spectral type M8 and drops sharply at late-M spectral types (e.g. West et al. 2004). The coronal X-ray emission levels of L dwarfs are generally below the current sensitivity limits (Stelzer et al. 2006). As the convection layer is deepening with the decreasing effective temperature the activity fraction of variability increase when the mass of stars decrease is expected.

## 5 DISCUSSION AND CONCLUSION

We have conducted a photometric survey of the globular cluster NGC 6397 in a search for variable stars. We analysed 8 391 light curves of NGC 6397 stars which lie in the lower part of the main-sequence in the colour-magnitude diagram, between magnitude 17 and 23 (465nm-filter) where are stars

of spectral types K and M. We identified 412 stars, reaching  $\sim 4.8 \pm 0.2$  per cent of variability with timescales between 0.004 and 2 d with 99.9% confidence level of variability to be real.

The relationship between the fraction of candidates to variables (with amplitudes variation greater than  $\pm 0.2$  magnitude) in function of the stellar mass of the NGC 6397 stars is shown in Fig. 9. From the curves it is observed that the fraction of the variation increases as the mass decreases. Hartman et al. (2011) also found the increased variability with decreased mass of the studied field stars. However, the stars that we observe are of low metallicity.

## ACKNOWLEDGMENTS

We thank the referee for important comments and suggestions. We thanks to ESO-VLT data program ID, support team. We acknowledge financial support from the Brazilian Institution CNPq and CAPES.

## REFERENCES

- Basri, G., Walkowicz, L. M., Batalha, N., Gilliland, R. L., Jenkins, J., Borucki, W. J., Koch, D., Caldwell, D., Dupree, A. K., Latham, D. W., Meibom, S., Howell, S., Brown, T. 2010, *The Astrophysical Journal Letters*, 713, L155
- Binney, J., & Merrifield, M. 1998, *Galactic astronomy / James Binney and Michael Merrifield*. Princeton, NJ : Princeton University Press, 1998. (Princeton series in astrophysics) QB857 .B522 1998
- Carretta, E., Bragaglia, A., Gratton, R., D' Orazi, V., & Lucatello, S. 2009, *Astronomy and Astrophysics*, 508, 695
- Cohn, H. N., Lluguer, P. M., Couch, S. M., Anderson, J., Cool, A. M., van den Berg, M., Bogdanov, S., Heinke, Craig O., Grindlay, J. E. 2010, *The Astrophysical Journal*, 722, 20
- Drilling, J. S., & Landolt, A. U. 2000, *Allen's Astrophysical Quantities*, 381
- Freeman, K., & Bland-Hawthorn, J. 2002, *ARA&A*, 40, 487
- Gershberg, R. E. 2005, *Studies in Applied Mathematics*, Hansen, B.M. S., Anderson, J., Brewer, J., Dotter, A., Fahlman, G.. G., Hurley, J., Kalirai, J., King, I., Reitzel, D., Richer, H. B., Rich, R. M., Shara, M. M., Stetson, P. B. 2007, *The Astrophysical Journal*, 671, 380
- Hartman, J. D., Bakos, G. Á., Noyes, R. W., et al. 2011, *The Astronomical Journal*, 141, 166
- Harris, W. E. 1996, *Astronomical Journal*, 112, 1487
- Heyl, J. S., Richer, H., Anderson, J., Fahlman, G., Dotter, A., Hurley, J., Kalirai, J., Rich, R. M. et al. 2012, *Astrophysical Journal*, 761, 51
- Kaluzny, J., Thompson, I. B., Krzeminski, W., & Schwarzenberg-Czerny, A. 2006, *MNRAS*, 365, 548
- Kaluzny, J., & Thompson, I. B. 2003, *The Astronomical Journal*, 125, 2534
- Kaluzny, J. 1997, *Astronomy and Astrophysics Supplement Series*, 122, 1
- Kaluzny, J. 1996, *Astronomy and Astrophysics Supplement*, 120, 83

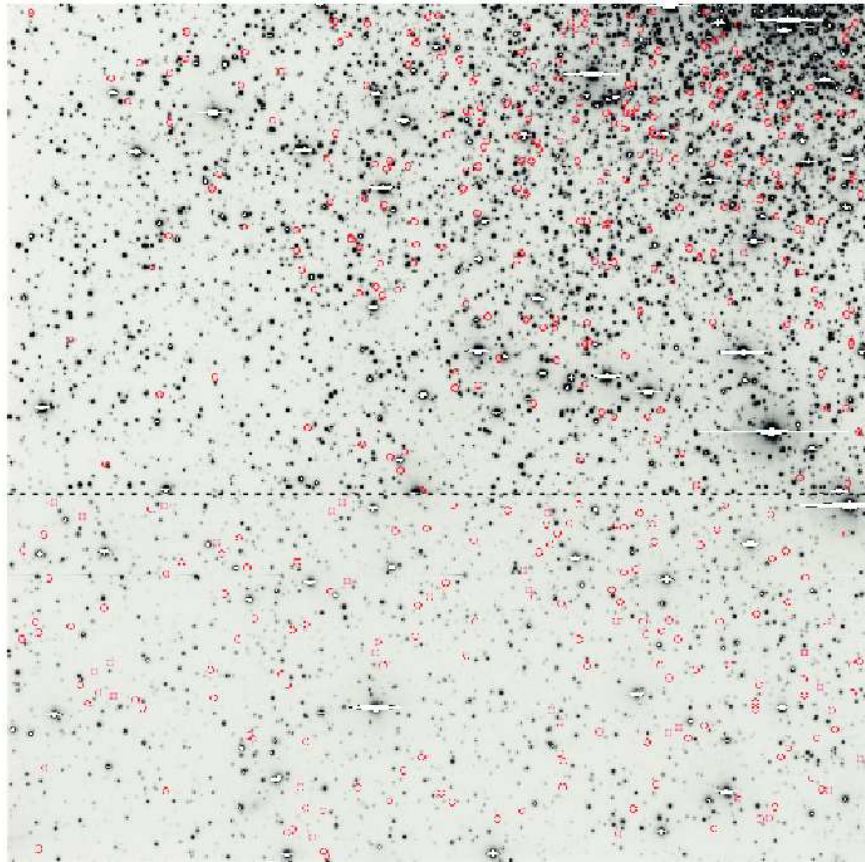


**Figure 7.** The circles show the positions of variables in images obtained with the ESO-VLT. Above and below CCD1, CCD2. The dashed line shows the boundary between the two CCDs.

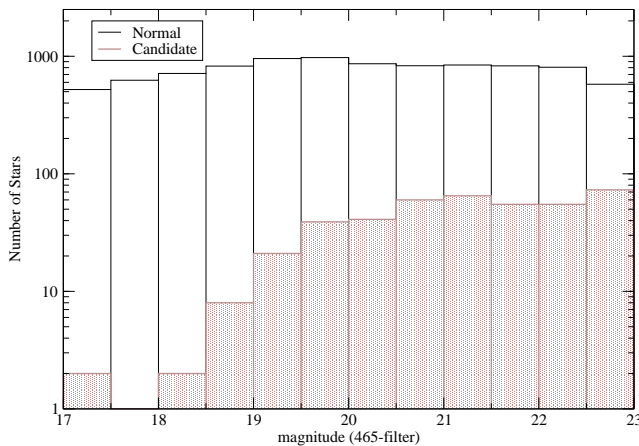


**Figure 8.** Magnitude distribution with the number of normal stars and magnitude with the number of variables stars candidate.

- Martinazzi, E., Pieres, A., Kepler, S. O., Costa, J. E. S., Bonatto, C., Bica, E. 2014, MNRAS, 442, 3105  
 Moehler, S., Heber, U., Napiwotzki, R., Koester, D., & Renzini, A. 2000, Astronomy & Astrophysics, 354, L75  
 Nascimbeni, V., Bedin, L. R., Piotto, G., De Marchi, F., & Rich, R. M. 2012, Astronomy & Astrophysics, 541, A144  
 Newton, E. R., Irwin, J., Charbonneau, D., Berta-Thompson, Z. K., Dittmann, J. A., West, A. A. 2015,

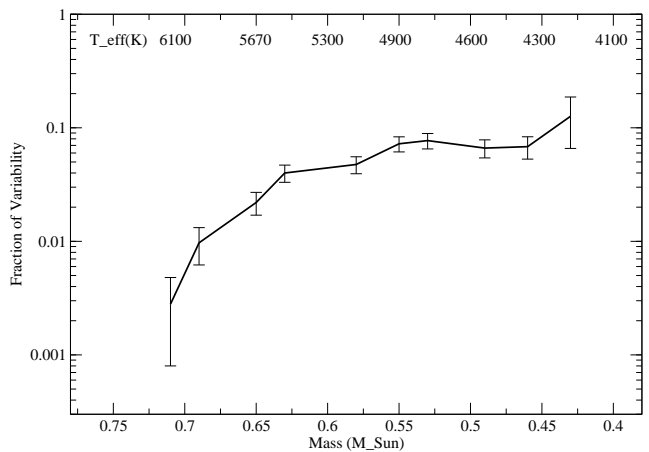


**Figure 9.** Fraction of candidates to variable in function of the stellar mass for NGC 6397 with magnitude between 17 and 23 (465nm-filter). The mass were estimated from the by isochrones calculated by A. Dotter (2008). The uncertainty bars are including the correction of uncertainty in completeness.

arXiv:1511.00957

- Rodríguez-López, C., MacDonald, J., Amado, P. J., Moya, A., & Mullan, D. 2014, MNRAS, 438, 2371  
 Rojas-Ayala, B., Iglesias, D., Minniti, D., Saito, R. K., & Surot, F. 2014, A & A, 571, A36

- Rosenberg, A., Piotto, G., Saviane, I., & Aparicio, A. 2000, *Astronomy and Astrophysics Supplement Series*, 144, 5
- Schmidt, S. J., Hawley, S. L., West, A. A., et al. 2015, *The Astronomical Journal*, 149, 158
- Stelzer, B., Micela, G., Flaccomio, E., Neuhauser, R., & Jayawardhana, R. 2006, *Astronomy and Astrophysics*, 448, 293
- Stetson, P. B. 2000, *Publications of the Astronomical Society of the Pacific*, 112, 925
- Stetson, P. B., Catelan, M., & Smith, H. A. 2005, *Publications of the Astronomical Society of the Pacific*, 117, 1325
- Trager, S. C., King, I. R., & Djorgovski, S. 1995, *Astronomical Journal*, 109, 218
- Valio, A. 2012, *IAU Symposium*, 286, 307
- Xiong, D. R., Deng, L., Zhang, C., & Wang, K. 2016, *Monthly Notices of the Royal Astronomical Society*, 457, 3163
- West, A. A., Hawley, S. L., Walkowicz, L. M., et al. 2004, *The Astrophysical Journal*, 128, 426
- West, A. A., Weisenburger, K. L., Irwin, J., Berta-Thompson, Z. K., Charbonneau, D., Dittmann, J., Pineda, J. S. 2015, *The Astrophysical Journal*, 812, 3

## 6 APPENDIX

The stars identified (ID) is compared by the CCD number (1 or 2) and the ID provides by IRAF, the coordinates (R.A. and Dec. for J2000), reduced Chi-square [ $\chi^2_{\text{red}} = \chi^2/(N-1)$ ], the average magnitude in the B\_HIGH, V\_HIGH and FILT\_465\_250 filters of the identified variable stars in NGC 6397 are listed in Table 1. Some stars we did not get the magnitudes of some filters.

**Table 1.** Variable stars in NGC 6397 with 99.9% confidence level.

Star ID	R.A. (J2000) <i>h m s</i>	Dec. (J2000) ° , ′ , ″	$\chi^2_{\text{red}}$	$\langle \text{FILT\_465\_250} \rangle$	$\langle \text{B\_HIGH} \rangle$	$\sigma_B$	$\langle \text{V\_HIGH} \rangle$	$\sigma_V$
1/ 103	17:40:47.42	-53:45:11.61	1.59	22.81	23.56	0.05	22.05	0.03
1/ 114	17:41:02.70	-53:45:12.39	2.59	21.79	16.47	0.18	16.77	0.19
1/ 122	17:40:41.69	-53:45:07.80	2.57	21.37	21.37	0.07	20.43	0.08
1/ 224	17:40:41.69	-53:45:07.89	1.79	21.42	21.81	0.04	20.64	0.04
1/ 322	17:41:03.84	-53:45:05.49	1.94	22.48	22.61	0.08	21.31	0.06
1/ 515	17:40:53.86	-53:44:59.11	1.55	19.53	19.81	0.01	19.01	0.01
1/ 571	17:41:04.40	-53:44:58.59	2.49	22.32	22.73	0.08	21.20	0.04
1/ 651	17:41:03.41	-53:44:56.71	1.70	21.70	21.81	0.07	20.52	0.10
1/ 654	17:40:48.13	-53:44:56.57	2.32	22.71	23.15	0.05	21.83	0.03
1/ 814	17:41:05.67	-53:44:51.69	1.63	22.23	21.57	0.05	20.69	0.04
1/ 875	17:40:49.61	-53:44:49.05	1.40	23.00	23.63	0.04	22.07	0.02
1/ 1021	17:41:08.85	-53:44:43.53	1.54	23.00	23.71	0.06	22.11	0.03
1/ 1204	17:40:52.02	-53:44:37.78	2.01	22.62	23.21	0.06	21.99	0.05
1/ 1214	17:40:50.11	-53:44:37.77	1.92	22.68	23.86	0.08	22.16	0.04
1/ 1266	17:40:52.65	-53:44:36.53	2.07	22.96	23.10	0.04	21.81	0.03
1/ 1305	17:40:49.47	-53:44:34.63	1.96	22.71	23.30	0.07	21.67	0.04
1/ 1347	17:40:39.08	-53:45:10.90	1.97	21.74	21.77	0.06	20.48	0.06
1/ 1357	17:40:40.17	-53:44:34.02	1.40	19.16	19.51	0.01	18.74	0.02
1/ 1416	17:40:56.29	-53:44:31.87	2.29	22.19	22.29	0.08	20.90	0.06
1/ 1576	17:41:17.07	-53:44:25.80	1.83	22.99	24.16	0.07	22.58	0.04
1/ 1672	17:41:00.87	-53:44:24.35	1.35	22.36	22.90	0.04	21.37	0.03
1/ 1715	17:40:59.45	-53:44:22.85	1.44	21.62	21.96	0.02	20.82	0.03
1/ 1740	17:40:53.66	-53:44:22.08	1.89	22.12	22.67	0.05	21.26	0.03
1/ 1839	17:41:14.10	-53:44:20.55	2.37	22.66	24.69	0.14	22.98	0.08
1/ 1905	17:40:40.51	-53:44:15.96	1.53	22.06	23.13	0.07	21.81	0.07
1/ 1941	17:41:00.70	-53:44:16.08	2.23	22.45	23.27	0.09	21.88	0.06
1/ 2111	17:40:58.49	-53:44:10.81	2.84	22.96	20.73	0.10	19.83	0.24
1/ 2136	17:40:55.18	-53:44:10.80	1.76	23.00	23.57	0.05	22.33	0.05
1/ 2209	17:40:51.36	-53:44:08.32	1.85	22.74	23.09	0.05	21.72	0.02
1/ 2385	17:40:53.61	-53:44:02.89	1.86	20.36	21.18	0.08	20.08	0.12
1/ 2387	17:40:38.89	-53:44:01.56	1.30	20.96	21.36	0.02	20.27	0.03
1/ 2436	17:40:53.41	-53:44:01.38	2.19	22.94	21.97	0.07	20.48	0.06
1/ 2441	17:40:38.89	-53:44:02.77	1.71	21.11	21.49	0.02	20.36	0.03
1/ 2687	17:40:55.22	-53:43:54.73	1.75	22.69	22.84	0.05	21.33	0.03
1/ 2694	17:40:55.93	-53:43:54.43	1.89	22.57	23.29	0.06	21.65	0.02
1/ 2721	17:40:41.21	-53:43:53.72	1.49	22.71	23.39	0.07	21.94	0.03
1/ 2752	17:40:42.40	-53:43:52.83	1.55	22.04	22.41	0.04	21.11	0.03
1/ 2782	17:40:53.58	-53:43:52.30	1.32	21.10	21.91	0.06	20.60	0.04
1/ 2804	17:40:46.53	-53:43:51.96	1.38	21.84	22.62	0.04	21.10	0.03
1/ 2836	17:40:56.85	-53:43:50.50	2.17	22.35	22.59	0.04	21.14	0.03
1/ 2846	17:40:55.18	-53:43:50.80	2.63	22.45	23.06	0.12	21.68	0.10
1/ 2894	17:40:58.96	-53:43:49.61	1.56	22.89	23.36	0.06	22.05	0.06
1/ 2923	17:40:39.17	-53:43:48.23	1.79	22.71	23.51	0.03	22.02	0.02
1/ 3002	17:40:50.55	-53:43:46.45	2.03	20.40	20.76	0.01	19.78	0.01
1/ 3019	17:40:38.89	-53:43:45.72	2.06	21.45	21.63	0.03	20.51	0.03
1/ 3130	17:40:40.66	-53:43:43.23	2.07	22.29	22.79	0.12	21.42	0.02
1/ 3157	17:41:00.16	-53:43:42.72	2.75	22.28	23.25	0.09	21.72	0.05
1/ 3312	17:41:04.75	-53:43:38.32	1.83	21.85	22.07	0.03	20.80	0.02
1/ 3346	17:41:06.10	-53:43:37.69	1.99	22.90	23.40	0.07	21.92	0.03
1/ 3402	17:41:08.57	-53:43:35.81	1.35	22.36	22.80	0.03	21.68	0.02
1/ 3404	17:41:03.98	-53:43:35.82	1.36	22.75	23.55	0.06	21.98	0.02
1/ 3424	17:40:40.87	-53:43:35.70	1.34	22.46	22.96	0.05	21.53	0.03
1/ 3586	17:40:48.78	-53:43:31.39	2.42	19.49	20.31	0.04	19.29	0.04
1/ 3756	17:40:41.65	-53:43:26.93	1.59	22.22	22.50	0.03	21.14	0.02
1/ 3791	17:41:09.27	-53:43:25.77	1.50	22.94	23.63	0.05	22.07	0.02
1/ 3797	17:40:49.70	-53:43:25.75	1.30	20.88	21.13	0.01	20.06	0.02
1/ 3841	17:40:52.39	-53:43:24.51	1.66	21.16	21.42	0.02	20.29	0.03
1/ 3847	17:41:17.47	-53:43:23.84	2.15	19.99	20.34	0.02	19.56	0.03
1/ 3899	17:41:03.06	-53:43:23.28	2.54	21.50s	21.47	0.03	20.20	0.04
1/ 3908	17:41:04.89	-53:43:22.65	1.30	22.96	23.66	0.08	22.09	0.02
1/ 3950	17:40:53.09	-53:43:22.00	1.52	22.05	22.37	0.03	20.96	0.02

**Table 2.** Continuation.

Star ID	R.A. (J2000) <i>h m s</i>	Dec. (J2000) °, ′, ″	$\chi^2_{\text{red}}$	$\langle \text{FILT\_465\_250} \rangle$	$\langle \text{B\_HIGH} \rangle$	$\sigma_B$	$\langle \text{V\_HIGH} \rangle$	$\sigma_V$
1/ 3993	17:40:57.40	-53:43:20.76	2.46	22.84	23.22	0.06	21.68	0.03
1/ 3994	17:40:52.18	-53:43:21.37	1.91	22.24	22.59	0.11	21.27	0.10
1/ 4001	17:40:42.43	-53:43:19.42	1.73	19.45	20.50	0.04	19.72	0.13
1/ 4041	17:40:47.23	-53:43:19.46	2.51	21.36	22.16	0.05	20.95	0.07
1/ 4093	17:40:57.26	-53:43:18.26	1.39	19.20	19.57	0.01	18.80	0.01
1/ 4111	17:40:46.45	-53:43:18.20	1.95	20.65	21.29	0.05	20.33	0.07
1/ 4119	17:40:44.76	-53:43:18.18	2.73	22.98	22.08	0.07	20.22	0.12
1/ 4152	17:41:09.56	-53:43:16.99	2.63	22.50	22.50	0.03	21.07	0.03
1/ 4187	17:40:47.87	-53:43:15.70	1.83	22.98	23.68	0.06	22.08	0.03
1/ 4205	17:41:06.02	-53:43:15.12	2.29	20.63	20.44	0.17	19.52	0.03
1/ 4215	17:41:01.43	-53:43:14.50	1.76	21.75	22.72	0.06	21.45	0.06
1/ 4374	17:41:06.59	-53:43:09.48	1.61	22.98	23.46	0.11	21.99	0.08
1/ 4414	17:41:16.62	-53:43:08.80	2.77	22.68	22.54	0.08	21.31	0.07
1/ 4508	17:41:09.63	-53:43:06.96	1.42	21.58	21.97	0.03	20.72	0.03
1/ 4523	17:40:50.06	-53:43:06.94	2.01	20.72	20.77	0.02	19.59	0.02
1/ 4543	17:40:41.79	-53:43:06.24	1.51	22.87	23.56	0.05	22.00	0.03
1/ 4561	17:41:12.45	-53:43:05.06	2.04	22.63	22.86	0.04	21.51	0.03
1/ 4633	17:40:52.39	-53:43:03.81	1.86	20.55	20.83	0.03	19.86	0.03
1/ 4681	17:41:03.06	-53:43:02.58	1.35	22.96	23.61	0.03	22.03	0.02
1/ 4691	17:40:41.16	-53:43:02.47	1.69	21.80	22.17	0.05	20.97	0.05
1/ 4692	17:40:40.45	-53:43:01.84	1.55	21.71	22.41	0.04	21.09	0.02
1/ 4702	17:40:53.80	-53:43:01.94	2.47	22.90	23.88	0.09	22.24	0.04
1/ 4703	17:40:53.45	-53:43:01.94	1.35	22.83	22.80	0.05	21.29	0.04
1/ 4767	17:40:42.99	-53:42:59.98	2.40	22.53	23.14	0.05	21.92	0.04
1/ 4830	17:40:59.52	-53:42:58.82	1.75	20.26	20.60	0.06	19.58	0.06
1/ 4952	17:40:48.29	-53:42:56.27	1.86	22.10	22.47	0.04	21.36	0.03
1/ 4966	17:40:45.89	-53:42:55.62	2.45	22.66	23.36	0.14	22.00	0.09
1/ 4972	17:40:45.18	-53:42:54.99	1.86	21.80	21.37	0.07	20.24	0.10
1/ 5020	17:41:04.68	-53:42:54.43	2.23	21.91	21.76	0.07	20.65	0.04
1/ 5094	17:41:07.65	-53:42:51.91	1.37	21.80	22.15	0.06	20.92	0.05
1/ 5127	17:40:43.84	-53:42:51.84	2.17	22.64	22.79	0.08	21.23	0.07
1/ 5155	17:41:05.74	-53:42:51.29	1.41	19.76	19.88	0.01	19.04	0.01
1/ 5247	17:40:56.84	-53:42:50.66	1.37	22.30	22.88	0.05	21.47	0.04
1/ 5250	17:40:38.33	-53:42:49.27	1.49	22.69	23.64	0.06	22.04	0.03
1/ 5361	17:41:00.30	-53:42:46.28	1.33	22.52	22.96	0.04	21.59	0.02
1/ 5367	17:41:14.22	-53:42:46.24	1.58	22.81	22.94	0.06	21.65	0.03
1/ 5383	17:40:57.41	-53:42:45.65	2.28	22.99	22.98	0.05	21.39	0.04
1/ 5452	17:40:42.85	-53:42:44.30	3.10	19.47	20.08	0.07	19.14	0.07
1/ 5492	17:40:44.69	-53:42:43.07	1.82	22.39	22.26	0.05	21.26	0.08
1/ 5508	17:40:44.62	-53:42:43.07	1.56	21.27	21.45	0.04	20.33	0.03
1/ 5530	17:40:38.62	-53:42:43.00	1.39	20.86	21.24	0.02	20.15	0.01
1/ 5537	17:40:52.81	-53:42:43.12	1.90	22.30	22.72	0.05	21.42	0.04
1/ 5573	17:40:51.33	-53:42:41.23	1.65	19.41	19.84	0.02	19.02	0.02
1/ 5622	17:40:39.89	-53:42:40.51	1.39	19.20	19.34	0.01	18.62	0.01
1/ 5663	17:41:13.79	-53:42:39.34	2.12	22.46	22.76	0.03	21.32	0.02
1/ 5669	17:40:38.90	-53:42:38.62	2.22	21.06	22.00	0.06	20.76	0.07
1/ 5691	17:40:43.07	-53:42:38.66	1.31	21.77	22.50	0.07	21.30	0.05
1/ 5705	17:40:52.39	-53:42:39.36	1.54	20.38	20.88	0.03	19.84	0.02
1/ 5757	17:41:00.16	-53:42:37.50	2.28	19.45	19.94	0.03	19.17	0.11
1/ 5784	17:40:41.94	-53:42:36.77	2.43	22.47	22.55	0.05	21.01	0.03
1/ 5793	17:41:04.61	-53:42:36.24	2.12	21.27	22.25	0.04	21.12	0.04
1/ 5833	17:41:03.34	-53:42:35.62	1.74	22.68	23.43	0.07	21.85	0.02
1/ 5834	17:40:59.45	-53:42:35.62	1.67	22.09	22.68	0.04	21.23	0.02
1/ 5876	17:41:05.18	-53:42:34.36	1.41	22.05	22.42	0.05	21.08	0.04
1/ 5893	17:40:45.54	-53:42:34.30	1.33	21.67	22.17	0.02	21.04	0.02
1/ 5921	17:40:46.60	-53:42:33.68	2.06	22.19	22.46	0.03	21.10	0.03
1/ 5947	17:40:56.56	-53:42:33.10	1.55	20.87	21.45	0.05	20.32	0.03
1/ 5970	17:41:04.40	-53:42:33.11	1.44	20.06	20.92	0.03	19.92	0.02
1/ 5971	17:40:57.12	-53:42:32.48	1.68	20.40	20.59	0.02	19.46	0.02
1/ 5972	17:40:54.02	-53:42:32.47	1.50	22.92	23.65	0.04	22.10	0.02
1/ 5986	17:40:56.14	-53:42:26.83	1.58	22.74	23.22	0.07	21.87	0.04

**Table 3.** Continuation.

Star ID	R.A. (J2000) <i>h m s</i>	Dec. (J2000) °, ′, ″	$\chi^2_{\text{red}}$	$\langle \text{FILT\_465\_250} \rangle$	$\langle \text{B\_HIGH} \rangle$	$\sigma_B$	$\langle \text{V\_HIGH} \rangle$	$\sigma_V$
1/ 5987	17:40:43.63	-53:42:32.40	1.42	22.61	22.93	0.08	21.76	0.07
1/ 6005	17:41:07.86	-53:42:31.22	2.14	22.87	23.75	0.07	22.27	0.03
1/ 6033	17:40:49.50	-53:42:31.19	1.49	22.13	22.70	0.05	21.45	0.03
1/ 6077	17:40:45.68	-53:42:29.28	1.32	19.94	19.90	0.02	19.08	0.04
1/ 6086	17:40:50.56	-53:42:29.32	1.58	21.73	21.94	0.03	20.85	0.02
1/ 6111	17:40:45.75	-53:42:29.91	1.44	19.40	19.69	0.02	18.89	0.04
1/ 6177	17:40:49.78	-53:42:28.06	1.63	22.33	23.57	0.20	21.85	0.05
1/ 6214	17:40:56.06	-53:42:26.83	2.65	22.08	22.42	0.04	21.10	0.02
1/ 6243	17:40:59.17	-53:42:26.21	1.40	22.93	23.70	0.05	22.11	0.02
1/ 6341	17:40:56.28	-53:42:23.70	1.55	21.80	22.72	0.10	21.34	0.06
1/ 6363	17:40:49.28	-53:42:23.66	2.19	22.85	18.86	0.29	18.32	0.15
1/ 6389	17:40:58.96	-53:42:23.08	2.05	22.40	22.62	0.25	21.46	0.02
1/ 6399	17:40:55.01	-53:42:22.44	1.34	22.00	21.99	0.02	21.02	0.03
1/ 6467	17:40:57.48	-53:42:21.19	1.57	22.05	21.34	0.09	20.27	0.10
1/ 6523	17:40:42.79	-53:42:20.48	1.54	22.69	23.55	0.06	22.02	0.06
1/ 6529	17:41:01.15	-53:42:19.94	1.35	22.17	22.76	0.03	21.37	0.02
1/ 6550	17:41:07.36	-53:42:18.68	1.57	22.52	23.23	0.05	21.92	0.03
1/ 6658	17:40:49.78	-53:42:16.77	2.31	21.59	21.54	0.08	20.36	0.06
1/ 6679	17:40:45.68	-53:42:17.37	1.95	20.21	20.75	0.03	19.71	0.02
1/ 6688	17:40:48.51	-53:42:16.13	2.13	22.31	22.50	0.08	21.41	0.11
1/ 6691	17:40:41.66	-53:42:16.07	1.88	22.84	23.61	0.16	22.24	0.09
1/ 6764	17:40:46.39	-53:42:14.24	1.70	19.90	20.00	0.01	19.15	0.01
1/ 6775	17:40:51.97	-53:42:14.90	1.67	20.91	21.02	0.02	19.91	0.03
1/ 6776	17:40:51.69	-53:42:14.27	2.03	22.88	23.53	0.06	22.04	0.06
1/ 6778	17:40:43.42	-53:42:14.21	2.58	22.72	22.97	0.07	21.51	0.04
1/ 6791	17:41:16.55	-53:42:13.61	2.86	22.68	22.97	0.05	21.47	0.02
1/ 6812	17:40:59.31	-53:42:13.67	1.43	20.60	21.06	0.02	20.03	0.03
1/ 6848	17:41:10.82	-53:42:12.40	2.02	22.90	23.29	0.10	21.71	0.07
1/ 6866	17:40:56.77	-53:42:13.04	2.45	20.91	21.60	0.04	20.47	0.03
1/ 6891	17:40:42.44	-53:42:11.69	1.39	21.12	21.52	0.03	20.53	0.03
1/ 6913	17:40:49.85	-53:42:11.13	1.47	21.38	21.69	0.03	20.55	0.03
1/ 6931	17:40:40.74	-53:42:11.05	2.31	21.90	22.54	0.07	21.01	0.08
1/ 6946	17:40:38.90	-53:42:10.40	1.57	21.71	22.78	0.12	21.27	0.04
1/ 6987	17:40:51.33	-53:42:09.25	1.32	22.29	22.62	0.04	21.18	0.04
1/ 7001	17:40:52.46	-53:42:09.26	1.74	22.65	22.82	0.04	21.35	0.04
1/ 7018	17:40:39.54	-53:42:09.15	1.39	20.96	21.79	0.04	20.60	0.03
1/ 7028	17:40:59.81	-53:42:08.65	2.14	22.15	22.45	0.03	21.14	0.04
1/ 7052	17:41:00.09	-53:42:08.03	1.36	21.72	21.80	0.08	20.51	0.08
1/ 7111	17:40:59.38	-53:42:06.77	1.39	22.49	22.76	0.05	21.47	0.04
1/ 7112	17:40:57.20	-53:42:06.77	2.17	22.29	22.25	0.08	21.04	0.08
1/ 7140	17:40:50.77	-53:42:06.74	2.55	20.63	21.04	0.03	20.00	0.01
1/ 7151	17:40:43.92	-53:42:06.06	2.05	21.06	21.23	0.01	20.13	0.01
1/ 7164	17:40:42.79	-53:42:06.05	1.56	21.37	21.65	0.03	20.42	0.02
1/ 7175	17:40:46.56	-53:42:05.31	1.76	21.02	21.60	0.02	20.40	0.02
1/ 7218	17:40:53.88	-53:42:04.45	1.45	21.15	21.41	0.07	20.15	0.05
1/ 7224	17:40:42.37	-53:42:04.36	1.36	20.72	20.83	0.02	19.67	0.02
1/ 7229	17:40:57.94	-53:42:03.98	2.53	22.82	22.82	0.09	21.23	0.05
1/ 7238	17:41:18.80	-53:42:03.56	1.73	21.89	22.47	0.05	21.07	0.04
1/ 7243	17:40:51.41	-53:42:03.95	2.12	22.71	22.55	0.08	21.03	0.05
1/ 7281	17:40:49.73	-53:42:03.21	1.90	21.27	21.35	0.08	19.99	0.08
1/ 7378	17:40:43.97	-53:42:01.05	2.43	22.38	23.10	0.12	21.75	0.14
1/ 7392	17:40:46.12	-53:42:00.26	2.26	21.88	21.95	0.02	20.61	0.02
1/ 7407	17:40:44.89	-53:42:00.15	2.01	19.86	20.19	0.04	19.42	0.08
1/ 7466	17:40:44.04	-53:41:58.94	2.55	22.48	22.73	0.06	21.65	0.07
1/ 7486	17:40:47.79	-53:41:58.97	2.18	21.27	21.55	0.02	20.25	0.04
1/ 7501	17:40:46.08	-53:42:00.47	2.74	20.96	22.11	0.06	20.63	0.06
1/ 7536	17:40:56.27	-53:41:57.20	1.61	20.95	21.21	0.01	20.04	0.02
1/ 7548	17:40:41.11	-53:41:57.08	1.63	20.74	20.74	0.02	19.87	0.02
1/ 7587	17:40:46.82	-53:41:55.56	1.63	22.65	22.70	0.08	21.10	0.06
1/ 7590	17:41:12.65	-53:41:55.59	1.34	22.64	22.43	0.05	21.06	0.06
1/ 7593	17:41:05.65	-53:41:56.14	2.18	21.41	21.61	0.04	20.44	0.04

**Table 4.** Continuation.

Star ID	R.A. (J2000) <i>h m s</i>	Dec. (J2000) $^{\circ}, '$ "	$\chi^2_{\text{red}}$	$\langle \text{FILT\_465\_250} \rangle$	$\langle \text{B\_HIGH} \rangle$	$\sigma_B$	$\langle \text{V\_HIGH} \rangle$	$\sigma_V$
1/ 7630	17:40:51.24	-53:41:55.59	2.17	21.75	21.66	0.04	20.46	0.05
1/ 7644	17:40:51.00	-53:41:53.50	1.51	21.28	22.03	0.06	20.81	0.05
1/ 7732	17:40:59.67	-53:41:52.48	1.39	22.57	23.27	0.06	21.74	0.03
1/ 7743	17:41:19.76	-53:41:51.62	1.37	22.56	23.17	0.05	21.74	0.04
1/ 7751	17:40:55.08	-53:41:51.85	2.05	19.89	20.68	0.03	19.73	0.03
1/ 7782	17:40:46.05	-53:41:51.79	2.07	22.02	22.19	0.07	20.85	0.04
1/ 7811	17:41:01.44	-53:41:51.23	1.51	19.40	19.50	0.01	18.70	0.01
1/ 7813	17:40:45.83	-53:41:50.54	1.67	21.58	22.00	0.03	20.74	0.02
1/ 7854	17:41:16.55	-53:41:48.67	2.22	23.00	23.35	0.09	21.75	0.06
1/ 7881	17:41:10.27	-53:41:49.33	1.57	22.97	23.48	0.03	22.00	0.01
1/ 7892	17:40:46.96	-53:41:48.04	1.94	20.64	20.67	0.01	19.63	0.01
1/ 7967	17:40:44.63	-53:41:46.14	1.39	22.81	22.50	0.12	21.78	0.06
1/ 7975	17:40:56.43	-53:41:46.21	2.73	22.93	23.56	0.11	21.93	0.04
1/ 7983	17:40:43.36	-53:41:46.13	1.38	20.64	20.91	0.02	19.80	0.03
1/ 7993	17:41:03.35	-53:41:45.59	1.45	20.35	20.48	0.03	19.43	0.04
1/ 8023	17:40:39.16	-53:41:45.30	1.49	19.63	20.36	0.03	19.39	0.04
1/ 8037	17:41:18.20	-53:41:44.74	1.49	22.57	23.06	0.05	21.47	0.03
1/ 8047	17:40:49.96	-53:41:44.77	1.90	21.79	22.25	0.05	21.20	0.07
1/ 8102	17:40:55.04	-53:41:43.54	2.77	22.08	22.28	0.05	20.80	0.04
1/ 8115	17:41:00.55	-53:41:43.55	1.63	22.55	23.15	0.05	21.84	0.02
1/ 8137	17:41:15.66	-53:41:42.25	2.05	22.21	22.42	0.04	20.90	0.06
1/ 8153	17:41:01.54	-53:41:42.30	1.67	22.48	23.03	0.05	21.68	0.03
1/ 8258	17:40:44.95	-53:41:40.34	1.50	21.46	21.69	0.08	20.63	0.08
1/ 8274	17:41:01.47	-53:41:39.16	2.24	21.82	21.86	0.08	20.57	0.07
1/ 8285	17:41:12.34	-53:41:39.13	1.56	21.52	21.95	0.02	20.72	0.02
1/ 8290	17:40:57.16	-53:41:39.16	1.50	20.92	21.23	0.02	20.05	0.02
1/ 8310	17:40:49.54	-53:41:38.50	1.78	22.30	22.98	0.08	21.52	0.05
1/ 8350	17:40:45.37	-53:41:37.84	2.21	21.94	22.12	0.02	21.02	0.02
1/ 8419	17:40:47.00	-53:41:35.97	1.92	21.86	22.08	0.05	20.75	0.03
1/ 8452	17:40:51.37	-53:41:34.75	2.19	22.32	22.98	0.07	21.36	0.04
1/ 8465	17:41:02.95	-53:41:33.52	1.49	22.94	23.94	0.07	22.26	0.13
1/ 8492	17:41:07.05	-53:41:33.51	2.19	20.73	21.20	0.02	20.11	0.02
1/ 8507	17:40:53.07	-53:41:34.13	2.75	22.33	23.16	0.11	21.56	0.03
1/ 8529	17:40:46.36	-53:41:33.46	1.51	18.86	19.06	0.01	18.08	0.03
1/ 8572	17:40:39.16	-53:41:29.62	1.51	22.56	23.07	0.10	21.58	0.07
1/ 8622	17:41:01.26	-53:41:31.01	2.19	21.97	22.67	0.05	21.29	0.04
1/ 8639	17:40:45.87	-53:41:30.95	2.09	21.20	21.79	0.07	20.51	0.07
1/ 8674	17:41:06.55	-53:41:30.38	1.82	22.30	23.50	0.06	21.97	0.03
1/ 8718	17:41:15.80	-53:41:27.83	1.36	22.80	23.62	0.06	21.96	0.02
1/ 8732	17:40:39.16	-53:41:32.13	1.45	20.04	20.12	0.02	19.21	0.01
1/ 8760	17:40:54.83	-53:41:29.12	1.84	20.77	20.90	0.01	20.02	0.02
1/ 8775	17:40:50.60	-53:41:28.47	1.91	21.82	21.97	0.04	20.85	0.02
1/ 8817	17:40:54.13	-53:41:27.86	2.57	22.26	22.70	0.04	21.61	0.04
1/ 8850	17:40:56.74	-53:41:27.24	2.09	19.73	20.03	0.06	19.19	0.06
1/ 8890	17:40:58.79	-53:41:25.37	2.65	22.85	23.79	0.11	21.81	0.05
1/ 8920	17:40:53.63	-53:41:25.98	1.75	22.68	23.62	0.12	22.38	0.18
1/ 8926	17:40:38.67	-53:41:25.23	2.09	21.99	22.71	0.08	21.19	0.05
1/ 8932	17:41:05.64	-53:41:25.36	1.49	21.72	22.05	0.02	20.79	0.02
1/ 8963	17:40:54.34	-53:41:24.48	2.28	22.15	22.69	0.04	21.42	0.03
1/ 8982	17:41:07.39	-53:41:23.73	1.94	21.57	21.20	0.05	20.05	0.03
1/ 9056	17:41:02.22	-53:41:22.23	2.45	22.49	22.95	0.05	21.58	0.02
1/ 9078	17:40:51.12	-53:41:22.20	2.49	22.09	22.42	0.09	20.92	0.05
1/ 9145	17:41:24.24	-53:41:19.84	1.42	21.33	22.12	0.03	20.87	0.02
1/ 9175	17:40:53.66	-53:41:20.71	1.67	21.68	22.07	0.02	20.75	0.01
1/ 9187	17:40:49.85	-53:41:19.94	2.02	22.09	21.97	0.05	20.81	0.04
1/ 9519	17:41:20.12	-53:45:01.12	1.38	19.23	19.39	0.01	18.64	0.01
1/ 9647	17:40:38.38	-53:44:45.26	2.24	19.00	19.13	0.01	18.28	0.03
1/ 10089	17:41:22.15	-53:44:01.65	1.39	19.72	19.88	0.01	19.05	0.01
1/ 10271	17:40:45.51	-53:43:41.38	1.41	19.49	19.92	0.01	19.03	0.02
1/ 10750	17:40:52.47	-53:43:04.55	1.32	19.28	19.54	0.02	18.66	0.02
1/ 11485	17:40:51.46	-53:42:17.14	1.44	19.76	20.06	0.01	19.24	0.01

**Table 5.** Continuation.

Star ID	R.A. (J2000) <i>h m s</i>	Dec. (J2000) ° ′ ″	$\chi^2_{\text{red}}$	$\langle \text{FILT\_465\_250} \rangle$	$\langle \text{B\_HIGH} \rangle$	$\sigma_B$	$\langle \text{V\_HIGH} \rangle$	$\sigma_V$
1/ 11550	17:40:54.17	-53:42:12.63	1.46	19.33	19.42	0.01	18.61	0.02
1/ 11587	17:41:01.46	-53:42:10.39	1.31	19.24	19.43	0.01	18.67	0.01
1/ 11618	17:40:51.03	-53:42:09.61	1.86	19.56	19.74	0.02	18.90	0.03
1/ 11759	17:40:38.66	-53:42:00.47	1.57	19.69	19.77	0.03	18.87	0.02
1/ 12053	17:40:39.43	-53:41:45.43	1.34	17.28	16.78	0.03	16.22	0.01
1/ 12379	17:41:03.23	-53:41:30.51	1.38	19.30	19.81	0.01	18.73	0.02
1/ 12495	17:40:45.10	-53:41:25.92	1.35	18.39	17.53	0.09	16.95	0.11
1/ 12590	17:41:01.71	-53:41:22.23	1.63	19.15	19.33	0.01	18.61	0.01
1/ 12655	17:40:46.88	-53:41:19.92	2.57	19.91	19.65	0.03	18.95	0.02
2/ 714	17:41:08.12	-53:48:15.51	1.90	21.37	22.48	0.06	21.03	0.06
2/ 911	17:41:08.69	-53:48:08.25	1.42	20.00	24.21	0.06	22.52	0.02
2/ 969	17:40:51.82	-53:48:06.64	1.60	20.03	24.15	0.07	22.50	0.03
2/ 984	17:41:10.17	-53:48:06.41	1.50	19.79	24.10	0.08	22.38	0.03
2/ 1036	17:40:46.53	-53:48:04.49	1.92	21.46	25.49	0.21	23.91	0.06
2/ 1040	17:41:09.80	-53:48:04.24	1.85	21.34	25.21	0.16	23.66	0.04
2/ 1216	17:40:43.95	-53:47:59.78	1.46	19.86	23.74	0.05	22.38	0.03
2/ 1221	17:40:58.53	-53:47:59.31	1.75	21.31	25.62	0.33	23.88	0.06
2/ 1225	17:40:43.46	-53:47:59.79	1.86	21.38	25.34	0.18	23.42	0.03
2/ 1337	17:41:08.16	-53:47:55.55	1.35	21.07	25.98	0.32	24.26	0.09
2/ 1339	17:40:57.14	-53:47:55.34	1.31	20.53	24.97	0.14	23.32	0.03
2/ 1371	17:40:50.91	-53:47:54.67	1.31	19.63	23.59	0.06	22.16	0.02
2/ 1378	17:41:09.10	-53:47:54.09	1.31	21.08	25.18	0.15	23.50	0.03
2/ 1393	17:40:43.09	-53:47:53.98	1.44	21.04	25.47	0.19	23.42	0.04
2/ 1480	17:41:00.99	-53:47:51.30	1.36	21.47	25.74	0.25	24.16	0.06
2/ 1510	17:41:04.51	-53:47:50.53	1.45	21.66	25.59	0.21	24.04	0.06
2/ 1527	17:40:45.14	-53:47:50.34	1.43	17.61	21.09	0.02	20.04	0.02
2/ 1618	17:41:01.56	-53:47:46.94	1.67	20.79	24.89	0.11	23.11	0.02
2/ 1656	17:41:16.96	-53:47:45.96	1.38	21.28	25.39	0.20	23.79	0.04
2/ 1667	17:40:40.14	-53:47:45.64	1.84	20.60	24.88	0.10	23.17	0.03
2/ 1685	17:41:06.23	-53:47:44.34	1.83	21.40	25.48	0.23	23.82	0.05
2/ 1711	17:40:54.84	-53:47:44.11	1.41	20.79	24.86	0.11	23.24	0.03
2/ 1759	17:40:49.68	-53:47:42.70	1.32	21.69	25.58	0.21	23.93	0.04
2/ 1872	17:40:41.08	-53:47:39.47	1.54	21.29	25.73	0.26	24.13	0.06
2/ 1958	17:41:03.65	-53:47:35.66	1.38	21.11	25.26	0.14	23.67	0.04
2/ 1975	17:41:23.59	-53:47:33.11	1.34	19.98	24.33	0.07	22.61	0.07
2/ 2077	17:40:54.84	-53:47:31.41	1.44	19.11	22.93	0.04	21.54	0.02
2/ 2128	17:40:38.42	-53:47:30.40	1.83	20.23	24.31	0.09	22.76	0.04
2/ 2152	17:41:02.66	-53:47:29.14	1.46	20.85	24.95	0.18	23.13	0.03
2/ 2181	17:40:42.84	-53:47:30.03	1.74	21.52	25.78	0.30	23.72	0.04
2/ 2214	17:41:07.01	-53:47:27.27	1.86	21.17	25.78	0.24	24.91	0.13
2/ 2226	17:40:54.72	-53:47:27.78	1.37	20.53	24.77	0.13	23.05	0.03
2/ 2312	17:40:42.35	-53:47:24.59	1.41	20.16	23.93	0.05	22.44	0.02
2/ 2408	17:40:50.21	-53:47:22.01	1.59	21.44	25.69	0.23	23.83	0.04
2/ 2426	17:41:09.09	-53:47:21.43	1.59	20.20	24.34	0.08	22.71	0.06
2/ 2469	17:41:11.96	-53:47:19.56	1.37	19.61	23.66	0.04	22.11	0.02
2/ 2478	17:40:40.79	-53:47:19.51	1.30	21.03	25.58	0.21	23.84	0.07
2/ 2483	17:40:47.92	-53:47:19.85	1.38	21.11	25.33	0.21	23.55	0.05
2/ 2516	17:41:12.25	-53:47:18.47	1.88	19.64	23.30	0.07	21.99	0.03
2/ 2567	17:40:49.03	-53:47:17.30	1.35	20.88	25.13	0.14	23.62	0.04
2/ 2580	17:40:52.88	-53:47:16.91	1.63	21.45	25.81	0.25	23.79	0.05
2/ 2610	17:40:39.81	-53:47:15.88	1.52	20.68	24.75	0.09	22.95	0.03
2/ 2661	17:40:48.41	-53:47:14.40	1.84	20.89	24.56	0.09	23.14	0.04
2/ 2677	17:40:47.06	-53:47:14.05	2.04	20.75	24.65	0.11	23.19	0.04
2/ 2746	17:40:55.00	-53:47:12.17	2.46	20.85	24.90	0.23	23.23	0.06
2/ 2939	17:40:55.49	-53:47:06.36	1.59	20.33	24.44	0.08	22.77	0.03
2/ 2955	17:40:44.23	-53:47:02.45	2.01	21.13	24.90	0.12	23.29	0.04
2/ 2980	17:41:18.14	-53:47:04.93	1.82	20.94	25.15	0.14	23.43	0.04
2/ 3031	17:41:21.17	-53:47:02.68	1.33	20.23	24.73	0.10	23.02	0.03
2/ 3060	17:40:44.19	-53:47:06.08	1.96	20.40	24.07	0.07	22.74	0.03
2/ 3098	17:41:18.55	-53:47:00.56	1.40	20.41	24.54	0.08	22.90	0.03
2/ 3135	17:41:14.25	-53:46:59.92	1.39	21.59	25.85	0.28	23.99	0.05

**Table 6.** Continuation.

Star ID	R.A. (J2000) <i>h m s</i>	Dec. (J2000) °, ′, ″	$\chi^2_{\text{red}}$	$\langle \text{FILT\_465\_250} \rangle$	$\langle \text{B\_HIGH} \rangle$	$\sigma_B$	$\langle \text{V\_HIGH} \rangle$	$\sigma_V$
2/ 3156	17:41:19.69	-53:46:58.72	1.67	21.05	25.03	0.13	23.55	0.04
2/ 3171	17:40:41.45	-53:46:58.83	1.97	20.49	24.53	0.08	22.85	0.03
2/ 3213	17:40:38.71	-53:46:58.83	2.07	21.06	25.07	0.15	23.37	0.04
2/ 3214	17:41:20.59	-53:46:57.25	1.54	20.76	24.93	0.12	23.08	0.03
2/ 3314	17:40:40.63	-53:46:54.84	1.58	21.51	25.66	0.25	23.97	0.05
2/ 3340	17:41:10.11	-53:46:53.83	1.54	20.17	24.14	0.06	22.54	0.02
2/ 3344	17:41:21.58	-53:46:53.60	1.38	19.56	23.24	0.07	21.78	0.04
2/ 3352	17:40:43.99	-53:46:53.74	1.62	18.91	22.72	0.03	21.41	0.02
2/ 3443	17:40:41.53	-53:46:51.20	1.38	20.53	24.62	0.09	23.01	0.02
2/ 3466	17:40:48.94	-53:46:50.08	1.53	21.41	25.35	0.18	23.64	0.04
2/ 3498	17:41:11.83	-53:46:49.81	1.32	19.00	22.59	0.03	21.61	0.02
2/ 3534	17:41:10.44	-53:46:48.02	1.84	20.44	24.70	0.13	22.87	0.03
2/ 3575	17:41:20.75	-53:46:45.63	1.68	20.66	25.49	0.20	23.88	0.05
2/ 3605	17:40:47.47	-53:46:46.46	1.69	20.41	24.24	0.06	22.67	0.02
2/ 3608	17:41:14.37	-53:46:46.13	1.39	21.23	25.26	0.13	23.74	0.04
2/ 3658	17:40:53.53	-53:46:44.61	1.88	21.08	24.98	0.13	23.34	0.03
2/ 3673	17:41:04.79	-53:46:44.12	2.21	20.27	24.33	0.07	22.61	0.02
2/ 3676	17:40:49.47	-53:46:44.28	1.46	20.51	25.33	0.28	23.40	0.08
2/ 3678	17:40:45.63	-53:46:43.93	1.57	19.27	23.18	0.04	21.53	0.02
2/ 3709	17:41:19.98	-53:46:42.02	1.45	20.93	24.88	0.12	23.33	0.04
2/ 3733	17:40:38.46	-53:46:42.50	1.91	21.01	25.07	0.15	23.23	0.04
2/ 3815	17:41:00.20	-53:46:38.37	1.63	20.65	25.13	0.15	23.58	0.06
2/ 3864	17:41:05.24	-53:46:37.94	1.45	20.41	24.81	0.10	22.91	0.02
2/ 3866	17:40:41.45	-53:46:38.14	1.64	19.55	23.49	0.05	22.03	0.02
2/ 4018	17:41:05.07	-53:46:32.86	1.45	21.27	25.78	0.25	23.83	0.04
2/ 4054	17:40:48.45	-53:46:31.58	1.55	21.54	25.69	0.26	23.82	0.05
2/ 4056	17:41:24.80	-53:46:31.02	2.05	19.00	23.54	0.10	22.34	0.05
2/ 4059	17:41:12.85	-53:46:31.28	1.38	20.73	24.91	0.10	23.28	0.04
2/ 4063	17:40:53.98	-53:46:31.54	1.32	21.08	25.05	0.14	23.49	0.04
2/ 4109	17:41:02.98	-53:46:29.63	1.64	19.58	23.39	0.06	21.94	0.03
2/ 4164	17:40:50.21	-53:46:28.30	1.60	22.00	25.44	0.20	23.92	0.05
2/ 4167	17:41:23.86	-53:46:27.78	1.68	20.98	24.92	0.14	23.21	0.03
2/ 4205	17:40:49.27	-53:46:26.86	1.45	19.82	23.94	0.06	22.32	0.03
2/ 4219	17:41:09.78	-53:46:26.62	1.42	21.70	25.57	0.22	23.70	0.04
2/ 4292	17:41:22.10	-53:46:24.19	1.61	21.54	25.71	0.26	23.87	0.05
2/ 4321	17:41:09.04	-53:46:24.09	1.31	21.00	25.45	0.20	23.47	0.03
2/ 4356	17:41:24.06	-53:46:22.69	1.47	19.85	23.91	0.05	22.32	0.02
2/ 4372	17:40:50.41	-53:46:22.50	1.93	21.66	25.23	0.13	23.67	0.04
2/ 4374	17:40:46.20	-53:46:22.52	1.65	20.93	25.18	0.15	23.52	0.03
2/ 4379	17:40:59.75	-53:46:22.41	1.81	21.51	25.05	0.14	23.42	0.04
2/ 4390	17:40:51.89	-53:46:22.12	1.34	20.26	24.44	0.07	22.88	0.02
2/ 4393	17:40:40.22	-53:46:22.54	1.74	20.51	24.59	0.12	22.73	0.02
2/ 4413	17:40:48.98	-53:46:22.14	1.33	21.26	25.51	0.20	23.79	0.07
2/ 4426	17:41:11.90	-53:46:20.78	1.36	21.33	25.56	0.21	23.80	0.05
2/ 4508	17:40:44.07	-53:46:19.26	1.68	20.95	25.31	0.23	23.43	0.05
2/ 4617	17:40:49.35	-53:46:27.58	1.61	20.60	24.85	0.12	23.25	0.03
2/ 4663	17:41:06.34	-53:46:24.86	1.41	20.74	25.02	0.14	23.35	0.04
2/ 4706	17:40:42.39	-53:46:13.46	1.74	21.67	25.48	0.20	23.58	0.04
2/ 4715	17:40:51.68	-53:46:13.05	1.62	20.95	24.62	0.08	23.13	0.03
2/ 4798	17:41:02.24	-53:46:10.40	1.33	20.43	24.76	0.11	23.05	0.03
2/ 4799	17:40:56.43	-53:46:10.47	1.58	20.11	24.46	0.08	22.98	0.04
2/ 4839	17:41:13.58	-53:46:09.13	1.33	20.75	25.16	0.14	23.17	0.03
2/ 4907	17:41:07.77	-53:46:07.78	2.27	19.66	22.15	0.10	20.65	0.14
2/ 4919	17:40:56.76	-53:46:06.84	1.40	21.18	25.10	0.13	23.52	0.05
2/ 4920	17:40:52.13	-53:46:06.88	1.32	20.05	24.05	0.17	22.76	0.11
2/ 5028	17:41:01.34	-53:46:03.88	1.41	20.18	24.54	0.10	22.65	0.02
2/ 5080	17:41:06.78	-53:46:02.35	1.50	20.55	24.32	0.10	22.75	0.03
2/ 5107	17:41:23.32	-53:46:01.30	1.31	19.87	23.77	0.05	22.36	0.03
2/ 5126	17:40:41.37	-53:46:01.13	1.41	20.88	24.66	0.10	23.23	0.03
2/ 5176	17:41:16.77	-53:45:59.27	1.71	19.52	23.77	0.30	22.00	0.06
2/ 5211	17:40:51.43	-53:45:58.54	1.50	21.50	25.44	0.32	23.68	0.06
2/ 5232	17:40:57.08	-53:45:57.76	1.43	19.98	24.23	0.09	22.72	0.04

**Table 7.** Continuation.

Star ID	R.A. (J2000) <i>h m s</i>	Dec. (J2000) $^{\circ}, ^{\prime}, ^{\prime\prime}$	$\chi^2_{\text{red}}$	$\langle \text{FILT\_465\_250} \rangle$	$\langle \text{B\_HIGH} \rangle$	$\sigma_B$	$\langle \text{V\_HIGH} \rangle$	$\sigma_V$
2/ 5243	17:40:50.82	-53:45:57.09	1.69	19.18	23.11	0.06	21.75	0.02
2/ 5274	17:41:12.39	-53:45:54.64	1.52	21.09	25.90	0.27	23.88	0.06
2/ 5364	17:41:15.95	-53:45:53.12	1.33	21.36	25.34	0.17	23.66	0.04
2/ 5384	17:41:09.52	-53:45:53.24	1.43	19.58	23.62	0.07	22.21	0.04
2/ 5440	17:40:43.29	-53:45:52.05	1.60	19.34	23.41	0.07	22.12	0.05
2/ 5500	17:41:13.62	-53:45:49.90	1.98	21.47	25.31	0.17	23.39	0.06
2/ 5540	17:40:56.18	-53:45:48.70	1.38	20.78	24.80	0.10	23.07	0.03
2/ 5552	17:40:42.47	-53:45:48.06	1.65	20.44	24.59	0.09	22.92	0.03
2/ 5553	17:41:24.71	-53:45:47.48	1.41	18.91	22.87	0.04	21.46	0.02
2/ 5678	17:40:55.57	-53:45:45.07	1.60	21.00	25.28	0.18	23.64	0.04
2/ 5705	17:41:13.98	-53:45:43.36	1.37	18.38	22.14	0.07	20.62	0.08
2/ 5718	17:40:49.76	-53:45:43.31	1.54	21.15	25.22	0.15	23.58	0.04
2/ 5730	17:40:59.74	-53:45:42.85	1.52	20.93	25.20	0.18	23.35	0.04
2/ 5780	17:41:12.80	-53:45:41.20	1.74	20.67	24.59	0.11	23.11	0.04
2/ 5827	17:41:23.56	-53:45:39.88	1.35	19.00	22.89	0.04	21.53	0.01
2/ 5840	17:40:39.16	-53:45:40.08	1.51	17.49	21.20	0.02	20.17	0.02
2/ 5855	17:40:55.12	-53:45:39.27	1.87	20.00	23.95	0.06	22.32	0.02
2/ 5884	17:41:04.12	-53:45:38.44	1.63	20.05	24.03	0.05	22.58	0.04
2/ 5919	17:40:46.32	-53:45:37.88	1.79	20.28	24.51	0.11	22.72	0.02
2/ 5937	17:41:02.36	-53:45:37.01	1.33	21.34	25.87	0.31	23.72	0.04
2/ 5957	17:40:51.43	-53:45:36.40	2.21	21.30	25.51	0.23	23.59	0.08
2/ 6006	17:40:55.77	-53:45:34.91	1.92	20.15	24.58	0.10	22.75	0.03
2/ 6007	17:40:51.88	-53:45:35.67	2.27	20.86	25.39	0.25	23.82	0.11
2/ 6014	17:40:49.88	-53:45:34.60	1.96	21.76	25.23	0.19	23.73	0.06
2/ 6036	17:40:54.46	-53:45:34.56	1.44	19.77	23.91	0.07	22.26	0.02
2/ 6151	17:41:21.47	-53:45:30.86	1.81	20.26	24.45	0.09	22.66	0.02
2/ 6189	17:40:43.37	-53:45:30.27	1.62	19.73	23.95	0.05	22.24	0.02
2/ 6229	17:40:55.69	-53:45:29.11	1.49	19.67	22.59	0.10	20.96	0.09
2/ 6230	17:40:50.57	-53:45:29.51	1.41	20.27	24.36	0.07	22.65	0.02
2/ 6248	17:41:07.60	-53:45:28.59	1.50	20.06	24.26	0.09	22.52	0.06
2/ 6260	17:40:57.90	-53:45:28.36	1.39	20.76	25.01	0.16	23.24	0.03
2/ 6291	17:41:17.66	-53:45:27.32	1.84	21.15	25.44	0.24	23.68	0.09
2/ 6300	17:40:45.70	-53:45:27.36	1.50	21.12	19.50	0.01	18.71	0.00
2/ 6327	17:41:16.93	-53:45:25.88	2.17	21.70	25.51	0.24	23.78	0.06
2/ 6352	17:41:00.93	-53:45:25.78	1.80	20.80	25.35	0.23	23.37	0.09
2/ 6357	17:40:53.93	-53:45:25.13	2.18	20.19	24.79	0.20	22.82	0.03
2/ 6376	17:41:07.02	-53:45:24.25	1.31	20.23	24.68	0.17	22.78	0.04
2/ 6386	17:41:22.98	-53:45:23.93	1.70	20.07	24.17	0.07	22.43	0.02